PE Progress Report 2-71

# PRIMITIVE EQUATION MODEL PROGRESS REPORT

# DECEMBER 1970 RESULTS

Philip G. Kesel

Peter H. Hildebrand

FLEET NUMERICAL WEATHER CENTRAL

MONTEREY, CALIFORNIA

January 1971

Contents

## List of Tables

## List of Figures

# Primitive Equation Model Performance
## December 1970

1. December Climatology

Figures 5 and 6 contain the mean monthly sea-level pressure and 500-MB height distributions, respectively, for the month of December 1970.

In Figure 5, note the principal cyclone track in the Pacific, extending from Japan across Kamchatka (996 mbs) to the Gulf of Alaska (998 mbs). Centers in the Kamchatka area tended to be about six millibars deeper in December than in November. Gulf of Alaska lows were about nine millibars deeper in December. On the Atlantic side, one center (1003 mbs) was located just south of Greenland, with another center (999 mbs) in the Barents Sea. The Atlantic cyclone tracks were slightly different from those observed in November. In November, there was an intense low (999 mbs) near Scotland, but it contained troughs which extended both westward to Hudson Bay and northeastward to the Barents Sea.

The Asian high was stronger in December (1046 mbs) than in November (1038 mbs). Canadian highs tended to be about three millibars higher in December, also.

In Figure 6, the 500-MB mean troughs were located over Japan, along the U. S. West Coast, just off the U. S. East Coast (60 West), along a line from eastern Europe to the Moroccan Coast, and near 35 East. The northeast Atlantic contained fairly strong ridging because of persistent blocking activity.

In November, by comparison, the 500-MB troughs were near 15 West, 30 East, over the Sea of Japan, near 145 West (oriented NE-SW), and near 87 West.

## 2. Surface Pressure Error Patterns

The monthly mean 24-hour and 48-hour error patterns for all PE surface pressure progs in December 1970 are provided in Figures 1 and 2, respectively. Corresponding hemispheric RMSE scores for the 12-, 24-, 36-, 48-, 60- and 72-hour surface progs are given in Table 1. The 36-hour surface prog RMSE scores by land and sea regions are shown in Table 3.

In Figure 1, we note the positive bias areas over the eastern portions of Asia and the United States. Each pattern exhibits an extension eastward over the adjacent (warm) ocean. In Figure 2, observe that the 48-hour mean error over Alaska has not increased, but slight amplification is indicated over eastern United States.

The Pacific cyclones, though numerous and intense in December, were handled quite well in the first 24 hours, but 4-8 millibars overdevelopment generally occurred in the 24-48 hour forecasts. In the Atlantic, no systematic bias was observed with the major storms, but the Pacific storms were handled better than their Atlantic counterparts. Storms in the Barents Sea region and in the Mediterranean were generally too deep (by about 3-5 millibars in 48 hours).

In Table 1, we record the forecast change, actual change and forecast error. (These are not additive.) Note that the PE Model is more courageous (it predicts more change than the SLP). Further, the amount of change it predicts is very close to the actual change (in the RMS sense). On the other hand, the PE forecast errors are considerably lower than the SLP. Note that the 72-hour PE forecast has more skill than a 48-hour SLP. As in November, every 72-hour PE surface prog contained skill over persistence.

In Table 3, we indicate the scores by geographical regions. Note that the PE contained twice the skill of the SLP in the Atlantic (compared to persistence) and about three times as much skill in the Pacific. In spite of this, we are confident that many of the systematic errors can be significantly reduced in the coming months.

3. Error Patterns at 500 MBS

The monthly-mean error patterns for 500 MB PE 24-hour and 48-hour progs are provided in Figures 3 and 4, respectively. The corresponding hemispheric RMSE scores for the 12-, 24-, 36-, 48-, 60- and 72-hour 500 MB progs are shown in Table 2. The 36-hour 500 MB prog RMSE scores, by regions, are shown in Table 4. As in the case of the mean error patterns at sea level, the 500 MB patterns show positive bias over the eastern portions of both Asia and the United States. Negative bias regions are in the northern portions of the Pacific and Atlantic. With one exception, the error patterns at sea level appear to be highly correlated with those at 500 MBS, as would be expected with an integrated multi-layer model. The anomaly occurs over Africa, where systematic negative errors at 500 MBS are not accompanied by a similar pattern at sea level.

In Table 2, observe that both the BARO and the PE are not forecasting enough change. The height progs tend to be evenly matched for the first 24 hours, but the PE upper-air progs get increasingly better as the forecast period lengthens. Table 4 indicates that both models did well in the 36-hour time frame. The European area was particularly changeable during December (95.2 meters RMS change), but a large part of this was predicted well. Height variability in the Near East and Indian Ocean regions was quite small, and both models had a tough job beating persistence.

4. Problem Areas

a. Flows over Mountains

Each 36-hour PE 500 MB prog in the month of December was compared to its verification analysis. After examining all of the notes on these results, a pattern emerged.

During periods when a 500 MB ridge was located over the Asian mountains, the downstream trough (over Japan) was generally 40 to 60 meters too weak. When a trough was located over the Asian mountains, the downstream ridge (over Japan) was generally 40 to 60 meters too strong.

The same observation was made with respect to features downstream of the Rocky Mountains (along the U. S. East Coast). Thus, the positive anomalies along the east coasts of Asia and the United States.

One possible explanation for this is that the mountains are reducing the zonal component of the flow a little too much, permitting export of mass northward downstream of mountains. In any event, it is one of the most difficult problems in numerical prediction to simulate the geostrophic adjustments of mass and motion fields around and just downstream of mountain ranges.

This is not the entire story concerning the east coasts of continents. Other factors are discussed in the following paragraphs.

b. Over-Development of Highs

Considering the 24-hour error pattern in Figure 1, we note positive bias regions over eastern Asia and eastern United States. Each pattern contains an extension over the adjacent (warm) ocean.

As we noted previously (November results), these positive areas are indicative of the tendency to over-develop continental highs. Three reasons are offered for this. The model does not presently contain <u>heat storage terms</u> for the underlying surfaces. In the autumn, the

underlying surface is somewhat warmer than southward-moving cold highs. One study by Sellers indicates that the lowest layers of these air masses are heated about 0.6 degrees Celsius per day from this source. Now, by midwinter, this source will become negligible. In late spring, the reverse is true. Secondly, the model does not contain the divergent component of the initial winds.

The extension of the positive bias seaward is another problem, resulting mainly from our inability to simulate the proper amount of sensible heat exchange. This is related to the way in which the temperature lapse rate must be modelled (in both the analyzed and predicted structures). In the analysis structure, an effective constant lapse rate is assigned to the lowest layer (1000 mbs - 775 mbs). In the prediction model, an effective temperature lapse rate is carried for the lowest one-fifth of the atmospheric column. The difficulty this poses with representing shallow stable layers (inversions) is quite obvious. The result, of course, is that the air-surface temperature difference required for sensible heat flux computations is underestimated. Thus, highs tend to be moved off-shore slightly too fast, and maintained too strong.

Finally, we noted earlier that the divergent wind component is not yet included in the specification of the initial winds.

As of 5 January 1971, the surface pressure progs have been subjected to a negative vorticity limiter (ellipticizor) to reduce the over-development of continental highs. Recent verifications indicate that a good part of this problem has been removed by this procedure. Keep in mind, however, that we are treating symptoms with an ellipticizor.

c. Truncation Error

The truncation error is proportional to both the mesh size of the computational grid and the scale size of the feature being simulated. It also depends on the way the finite-difference gradients are being calculated.

In the large scale features (SL), this factor is negligible. In the smaller scales (SD), however, the error increases as the scale of the feature decreases. For the most SD features, we tend to under translate by about 15 percent of observed displacement. The associated (SD) kinetic energy losses appear to be slight in the early portion of the forecast, but tend to accelerate with time. In other words, the under translation amounts to about 5-10 percent in the first 24 hours, 10-15 percent in the second 24 hours, and 15-25 percent in the final 24 hours.

Two remedies are possible, but only the second is likely to occur in the next year. First, we can shift to a better approximation to the finite-difference gradients (derivatives), most likely to fourth order vice second order. Secondly, we could shift to a finer-mesh grid, but this would lead to an unacceptable increase in the running time of the model (using our present computers).

d. Soft Boundary Problems

Recall that the model outputs a persistence forecast south of 4 North, a dynamic forecast north of the soft, internal boundary (this was located at 17 North until 1-26-71, then moved to 11 North), and a blend in between.

We have noticed (from mean error calculations by latitude bands) that the model has a positive bias of about 1-2 millibars per 72-hour forecast in the sub-tropics. Occasionally, a polar high does in fact surge southward. In any event, the return to climatology in data voids in the tropics and sub-tropics in (subsequent) analyses is rather severe*. This combination of circumstances has led to unrealistic gradients on the south side of low-latitude highs.

---

*As we "go to press" on this note, we find that the use of an ellipticizor to reduce highs has been a major factor in the generation of these fictitious peripheral gradients. Corrective action is being taken.

Two programs are affected directly: the wave/swell program, and the objective fronts program. In the former, fictitiously high wave/swell bands are being generated around the latitude band encompassing the soft boundary. In the frontal prog, fictitious fronts are being produced by the associated cusp in the meridional thickness profile in these same latitudes.

e. Slight Over-Development of Lows

(This was discussed earlier.)

f. The Tropopause Problem

This is a five-layer model. The two upper levels tend to straddle the mid- and high-latitude tropopause. Consequently, we had to assume that the temperatures varied linearly-in-log p between these levels. The temperatures (densities), and heights are in error, therefore, at 250-, 200- and 150-millibars.

We are currently working on a scheme which will correct this deficiency (by parameterizing the tropopause from lapse rates above and below it). Users will be advised.

5. Precipitation Forecasts

The PE Model outputs accumulated precipitation forecasts each six hours during an operational 72-hour forecast run. Two types of precipitation processes are being modelled: the so-called "large-scale" condensation, and area-averaged convective scale condensation.

a. Large-Scale Precipitation

In this instance, the following description is offered. The pertinent equation, of course, is the moisture conservation equation. This includes mathematical terms which represent horizontal and vertical advection of water vapor, horizontal and vertical convergence/divergence of water, evaporation (moisture source), and condensation (moisture sink) of the two previously mentioned types.

The initial moisture distribution is (presumably) known from the FNWC analyses of the vapor pressure at the surface, and the dewpoint depression analyses for levels up through 500 MBS. During the time integration of the primitive equations, each "unit cube" in the horizontal and vertical gridded space either gains or loses water vapor content as a consequence of the changes in the mass and motion fields, as specified by the previously mentioned moisture-content altering processes. Whenever the relative humidity exceeds 100% in any unit cube, condensation occurs. If condensation occurs at an upper level (cube), then each level (cube) beneath it is tested to determine its moisture state. If it is also saturated, then the precipitation merely passes through it; if not, evaporation is permitted into that level (cube). The total amount reaching the ground is accumulated for each ten-minute time step.

b. Convective-Scale Precipitation

Using an empirical approach taken by Mintz and Arakawa (in the UCLA general circulation model), we parameterize the presence of three types of cumulus clouds using measures of such quantities as: the conditional stability of the atmospheric column, the upward convective mass flux, some estimate of the incloud-environment temperature difference, and the like. Precipitation is allowed from two of the three cloud types thus modelled.

In addition to producing moderate amounts of convective rainfall, these terms have an additional purpose. They tend to redistribute heat and moisture between and out of the lowest three layers in the five-layer mode. Since this is an empirical technique, periodic tuning will be necessary.

Because of the use of internal "soft" boundaries (the constant flux, restoration boundary conditions developed locally) in the PE Model, it is necessary that evaporation and condensation be "turned off" south of the latitude where the soft internal boundaries are located. Elsewhere, we

have found the rainfall patterns to be representative of the observed area-averaged amounts. Keep in mind that individual observing stations will sometimes receive (possibly) two or three times the convective rainfall that is predicted using this approach.

This is still an experimental product. There are obvious shortcomings in the initial moisture analyses because of the sparse data coverage over oceans. If we receive integrated moisture fields from satellites in the future (a product that has been promised), then it will be very helpful indeed. In the meantime, comments are invited.

TABLE 1

VERIFICATION RESULTS OF DECEMBER 1970 SURFACE PROGNOSES

(in Millibars)

| FORECAST PERIOD (HOURS) | FORECAST CHANGE | | ACTUAL CHANGE | FORECAST ERROR | |
|---|---|---|---|---|---|
| | SLP | PE | | SLP | PE |
| 12 | 2.8 | 4.6 | 4.3 | 3.3 | 3.0 |
| 24 | 5.2 | 7.3 | 6.7 | 5.6 | 4.6 |
| 36 | 6.7 | 8.5 | 8.2 | 7.6 | 5.9 |
| 48 | 8.2 | 9.4 | 9.0 | 8.9 | 7.1 |
| 60 | 9.2 | 10.0 | 9.7 | 9.9 | 7.8 |
| 72 | 10.2 | 10.5 | 10.2 | 11.4 | 8.6 |

NOTE: RMSE scores are computed for all grid points north of 20° North. The inclusion of tropical points would make these figures considerably smaller.

TABLE 2

VERIFICATION RESULTS OF DECEMBER 1970 500 MB PROGNOSES

(in Meters)

| FORECAST PERIOD (HOURS) | FORECAST CHANGE | | ACTUAL CHANGE | FORECAST ERROR | |
|---|---|---|---|---|---|
| | BARO | PE | | BARO | PE |
| 12 | 34.7 | 38.5 | 43.8 | 29.0 | 31.4 |
| 24 | 56.4 | 59.3 | 67.1 | 45.9 | 44.3 |
| 36 | 68.9 | 73.3 | 82.3 | 59.4 | 56.7 |
| 48 | 80.5 | 82.4 | 90.7 | 70.5 | 65.9 |
| 60 | 91.6 | 89.6 | 98.0 | 87.9 | 77.7 |
| 72 | 97.5 | 95.4 | 108.2 | 97.7 | 82.8 |

NOTE: RMSE scores are computed for all grid points north of 20° North. The inclusion of tropical points would make these figures considerably smaller.

TABLE 3

VERIFICATION RESULTS OF DECEMBER 1970 36-HOUR PE MODEL

SURFACE PROGNOSES

| AREA | RMSE (millibars) | | |
|---|---|---|---|
| | Persistence | PE Model | SLP |
| NORTHERN HEMISPHERE (EQUATOR TO POLE) | 5.7 | 4.3 | 5.3 |
| LAND POINTS | 6.5 | 5.2 | 6.2 |
| SEA POINTS | 5.2 | 3.7 | 4.6 |
| LAND REGIONS: | | | |
| Americas | 8.0 | 5.8 | 7.6 |
| Asia | 6.9 | 5.8 | 6.7 |
| Near East | 2.1 | 2.2 | 2.2 |
| Europe | 7.8 | 5.1 | 6.5 |
| OCEAN REGIONS: | | | |
| Atlantic | 6.1 | 4.1 | 5.1 |
| Pacific | 4.8 | 3.4 | 4.4 |
| Indian | 2.3 | 2.0 | 2.3 |
| Mediterranean | 4.0 | 3.9 | 3.9 |

NOTES: (1) These figures are not comparable to those in Table 1 because Table 1 statistics apply to grid points North of 20°N only.

(2) The PE progs are used as the guess fields for surface pressure analyses.

TABLE 4

VERIFICATION RESULTS OF DECEMBER 1970 36-HOUR PE MODEL

500-MB PROGNOSES

| AREA | RMSE (Meters) | | |
|---|---|---|---|
| | Persistence | PE Model | Baro |
| NORTHERN HEMISPHERE (EQUATOR TO POLE) | 58.3 | 40.0 | 43.2 |
| LAND POINTS | 63.9 | 47.8 | 48.3 |
| SEA POINTS | 54.9 | 36.7 | 39.3 |
| LAND REGIONS: | | | |
| Americas | 76.1 | 51.3 | 57.5 |
| Asia | 62.9 | 44.0 | 48.0 |
| Near East | 28.8 | 29.8 | 25.2 |
| Europe | 95.2 | 53.8 | 59.9 |
| OCEAN REGIONS: | | | |
| Atlantic | 64.6 | 40.5 | 41.3 |
| Pacific | 50.7 | 35.1 | 38.4 |
| Indian | 19.4 | 17.1 | 17.3 |
| Mediterranean | 53.6 | 31.2 | 35.0 |

NOTES: (1) These figures are not comparable to those in Table 2 because Table 2 statistics apply to grid points North of 20°N only.

(2) The Barotropic Model's 500-MB height progs are used as guess fields for 500-MB analyses. PE Model 500-MB progs will be used for this purpose within a few weeks.

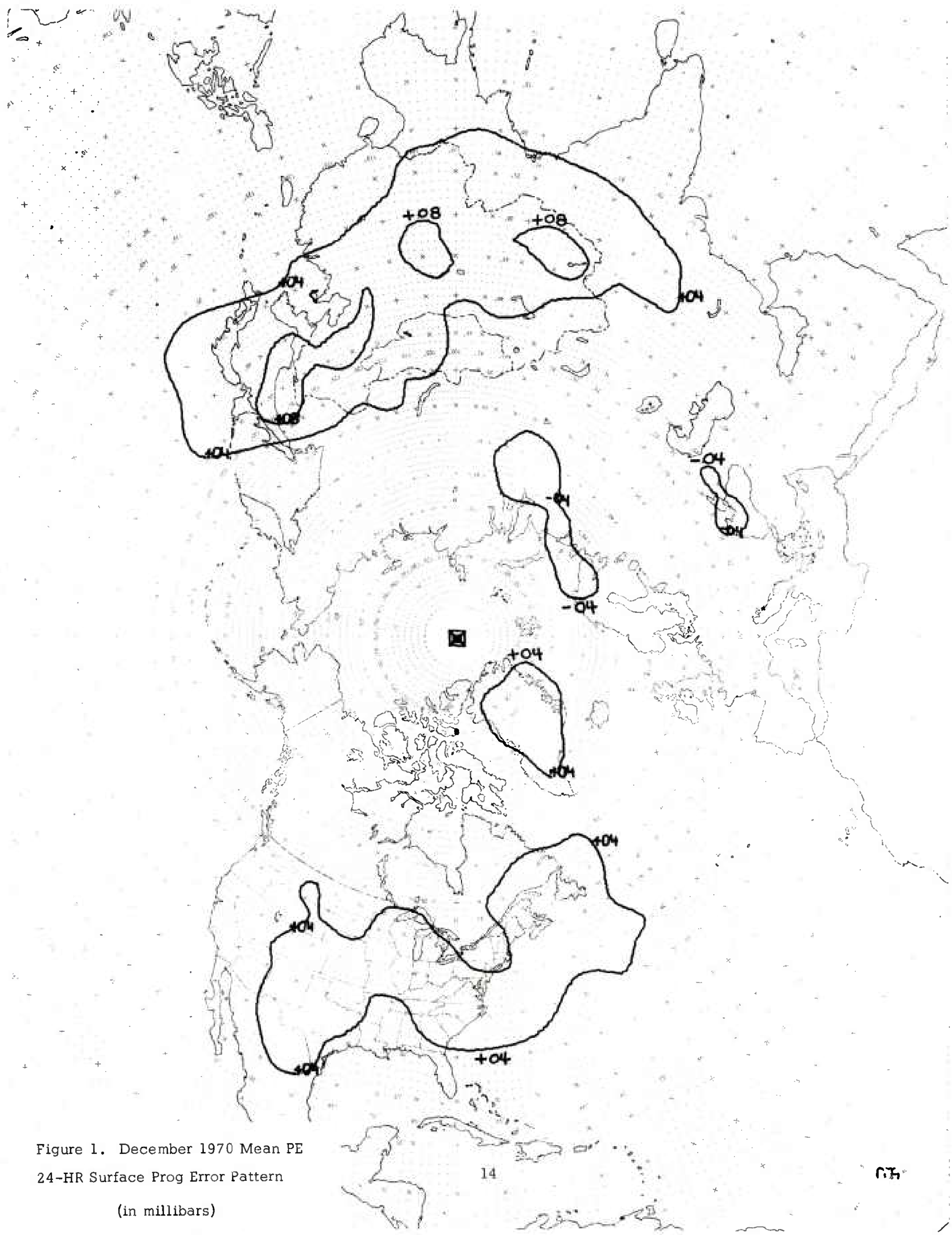


Figure 1. December 1970 Mean PE 24-HR Surface Prog Error Pattern (in millibars)


Figure 2. December 1970 Mean PE
48-HR Surface Prog Error Pattern
(in millibars)

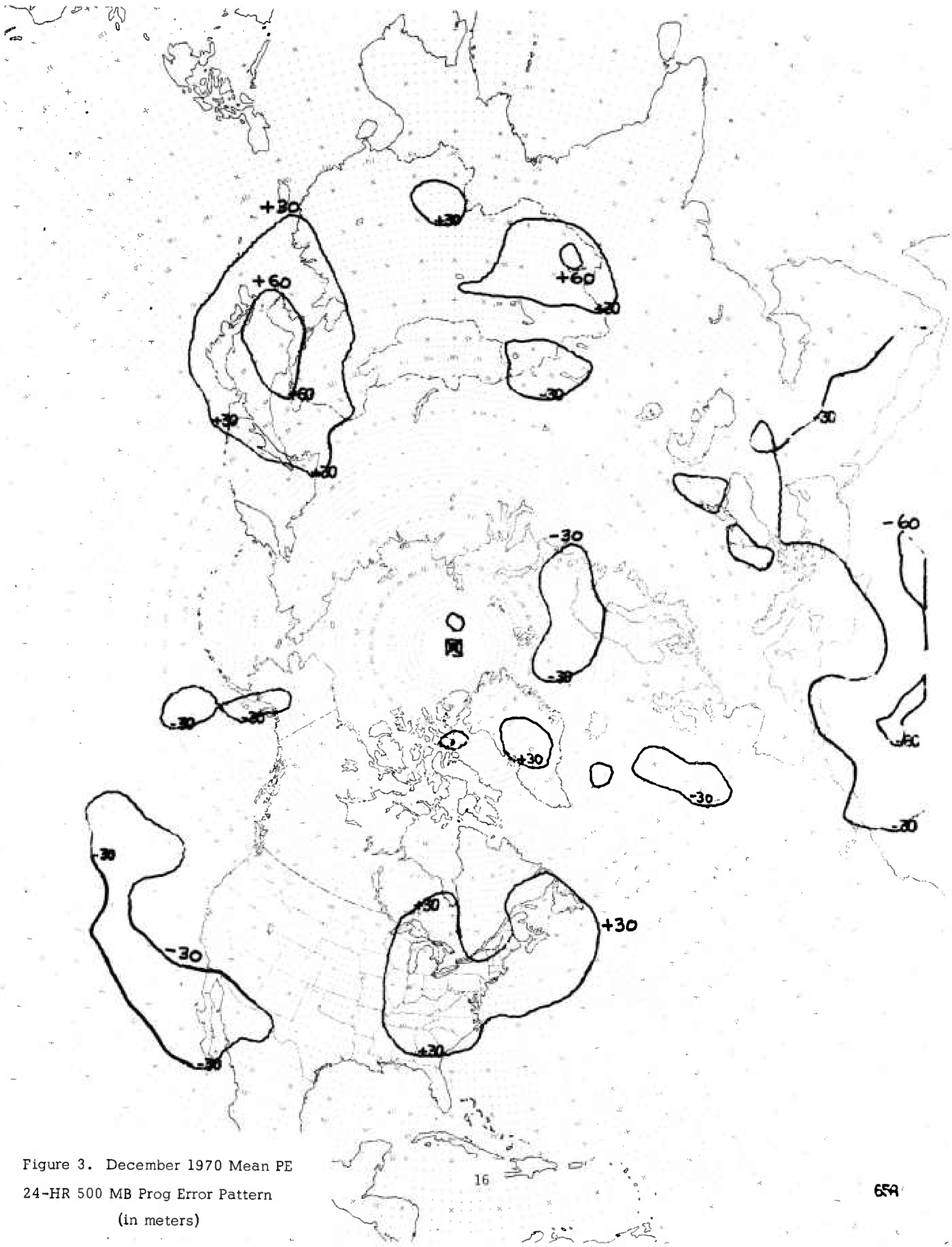


Figure 3. December 1970 Mean PE
24-HR 500 MB Prog Error Pattern
(in meters)



65A

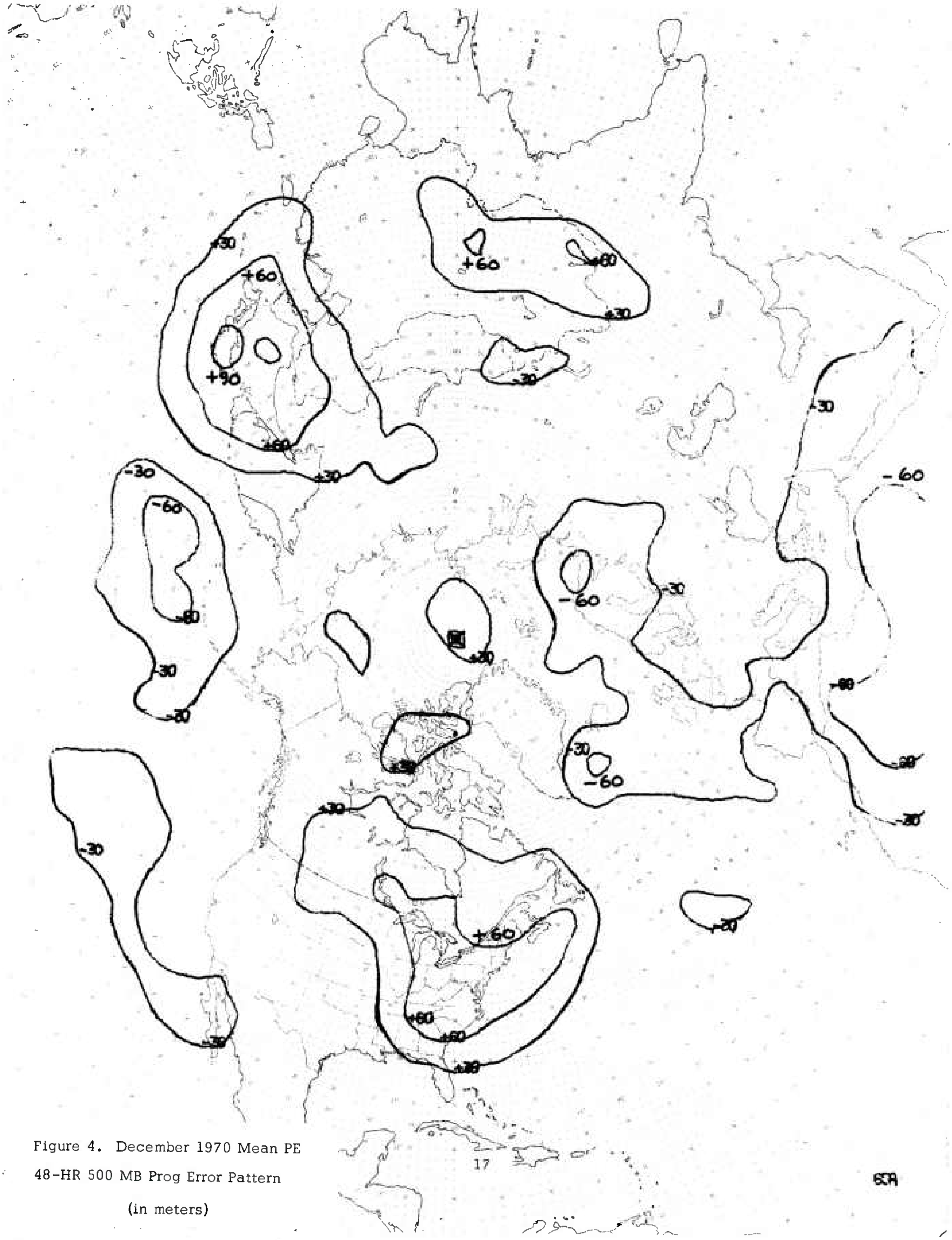


Figure 4. December 1970 Mean PE
48-HR 500 MB Prog Error Pattern
(in meters)



65A

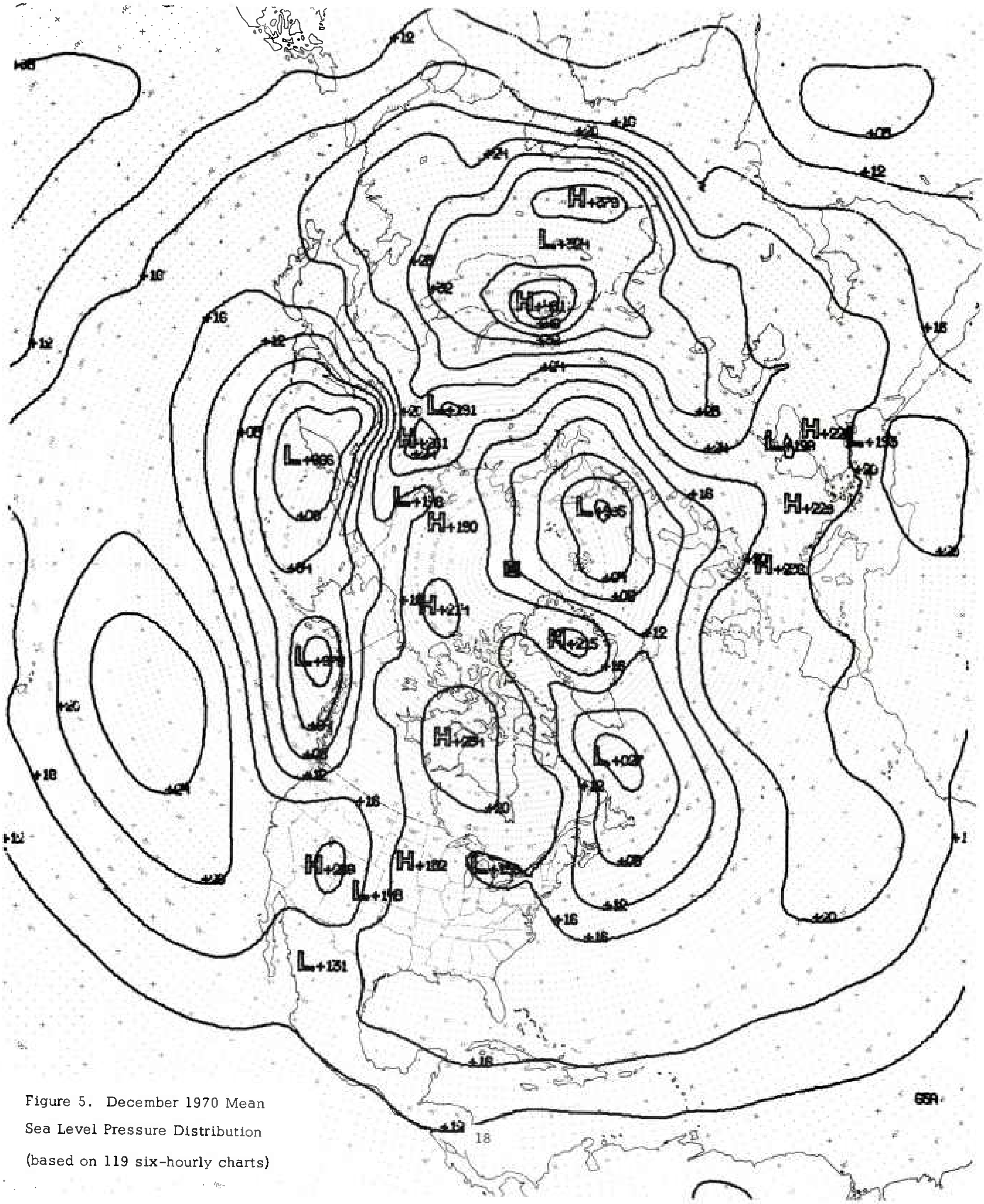

Figure 5. December 1970 Mean Sea Level Pressure Distribution (based on 119 six-hourly charts)

Figure 6. December 1970 Mean
500 MB Height Distribution
(based on 62 twelve-hourly charts)